

# Quantifying rapid changes in cardiovascular state with a moving ensemble average

Matthew Cieslak<sup>1</sup>  | William S. Ryan<sup>1</sup> | Viktoriya Babenko<sup>2</sup> | Hannah Erro<sup>2</sup> |  
 Zoe M. Rathbun<sup>2</sup> | Wendy Meiring<sup>3</sup> | Robert M. Kelsey<sup>4</sup> | Jim Blascovich<sup>5</sup> |  
 Scott T. Grafton<sup>5</sup>

<sup>1</sup>Department of Psychological and Brain Sciences, University of California Santa Barbara, Santa Barbara, California, USA

<sup>2</sup>Department of Psychological and Brain Sciences, University of California Santa Barbara, Santa Barbara, California, USA

<sup>3</sup>Department of Statistics and Applied Probability, University of California Santa Barbara, Santa Barbara, California, USA

<sup>4</sup>Memphis, Tennessee, USA

<sup>5</sup>Department of Psychological and Brain Sciences, University of California Santa Barbara, Santa Barbara, California, USA

## Correspondence

Matthew Cieslak, Ph.D, Department of Psychological and Brain Sciences, University of California, Santa Barbara, Santa Barbara, CA 93106, USA.  
 Email: matthew.cieslak@psych.ucsb.edu

## Funding information

General-Electric and the National Football League (Head Health Challenge grant), Institute for Collaborative Biotechnologies, U.S. Army Research Office (grant W911NF-09-0001), NSF (grants CCF-1525817 and CCF-1644747)

## Abstract

MEAP, the moving ensemble analysis pipeline, is a new open-source tool designed to perform multisubject preprocessing and analysis of cardiovascular data, including electrocardiogram (ECG), impedance cardiogram (ICG), and continuous blood pressure (BP). In addition to traditional ensemble averaging, MEAP implements a moving ensemble averaging method that allows for the continuous estimation of indices related to cardiovascular state, including cardiac output, pre-ejection period, heart rate variability, and total peripheral resistance, among others. Here, we define the moving ensemble technique mathematically, highlighting its differences from fixed-window ensemble averaging. We describe MEAP's interface and features for signal processing, artifact correction, and cardiovascular-based fMRI analysis. We demonstrate the accuracy of MEAP's novel B point detection algorithm on a large collection of hand-labeled ICG waveforms. As a proof of concept, two subjects completed a series of four physical and cognitive tasks (cold pressor, Valsalva maneuver, video game, random dot kinetogram) on 3 separate days while ECG, ICG, and BP were recorded. Critically, the moving ensemble method reliably captures the rapid cyclical cardiovascular changes related to the baroreflex during the Valsalva maneuver and the classic cold pressor response. Cardiovascular measures were seen to vary considerably within repetitions of the same cognitive task for each individual, suggesting that a carefully designed paradigm could be used to capture fast-acting event-related changes in cardiovascular state.

## KEYWORDS

analysis/statistical methods, autonomic, cardiovascular, fMRI, heart rate, impedance cardiography

## 1 | INTRODUCTION

Researchers from a variety of fields employ cardiovascular measurements to assess physiological and psychological states. Within noninvasive research on cardiovascular physiology, the most commonly employed methods of assessment are electrocardiogram (ECG), impedance cardiogram (ICG), and noninvasive continuous blood pressure (BP) monitoring. A variety of measures that have been used to index cardiovascular health and fitness (Matthews, Salomon, Brady, &

Allen, 2003), stress reactivity (Kelsey, Soderlund, & Arthur, 2004; Lovallo, 2005), motivational state (Blascovich, 2008; Seery, 2013; Wright, Contrada, & Patane, 1986), and emotion (Kreibig, Samson, & Gross, 2013) can be derived singularly and in concert from these data streams.

Innervated by the autonomic nervous system, the cardiovascular system responds dynamically to perturbations due to physiological and psychological stressors. Such responses can be necessarily fast acting, occurring on the order of seconds.

Current methods for processing and analyzing continuous ICG-based cardiovascular data, however, are not well suited to assessing such fast-acting changes. The most widely used data processing method in ICG-based cardiovascular research has long been the ensemble averaging technique (Kelsey & Guethlein, 1990). This technique is a reliable method for summarizing cardiovascular state during an experimental event. Ensemble averaging involves aligning the R peaks of each heartbeat within a given period of time, averaging the synchronized waveforms, and then marking the components of the ensemble averaged cardiac cycle to derive measures of interest. By averaging across cardiac cycles, the ensemble averaging method mitigates the impact of nonsystematic noise—respiratory and motion artifacts that are not synchronous with the R wave of the ECG. This method is advantageous as it requires annotation of only a single ensemble averaged heartbeat for each repetition of each experimental condition for each subject. Ensemble averaging precludes the need to manually annotate the ICG signal from every individual cardiac cycle, a laborious and error-prone process (Kelsey & Guethlein, 1990; Kelsey et al., 1998; Obrist, 1981). The robustness and efficiency of the ensemble averaging method (Kelsey & Guethlein, 1990; Kelsey, Ornduff, & Alpert, 2007; Kelsey et al., 2004) has made it an excellent tool for researchers studying cardiovascular activity.

The primary drawback of the ensemble averaging method is its limited ability to capture cardiovascular change within a window of time. Where cardiovascular changes occur and rebound quickly, these fluctuations may go undetected when a fixed-window ensemble averaging technique is applied. Depending on experimental design, these fluctuations may reflect meaningful and predictive differences in patterns of cardiovascular reactivity. Although ensemble averaging has been applied to very short blocks of time (Kelsey et al., 2004), the majority of psychophysiological studies have employed block designs with at least 30 s per trial. Moreover, using fixed-window ensemble averaging to detect phasic changes will only be accurate to the extent that the averaging window aligns with the timing of those phasic changes, which may not be known a priori.

Here, we present a new method for characterizing cardiovascular reactivity—moving ensemble averaging. The major innovation of this method is the ability to detect both state and change of cardiovascular indices during individual experimental trials. This technique is robust to respiratory and movement-related artifact normally present in noninvasive recordings as well as radio frequency and magnetic artifact present in an MRI environment (Cieslak et al., 2015). Open-source software implementing this technique as well as validation of its unique processing pipeline are presented. We chose to design an approach using Python and

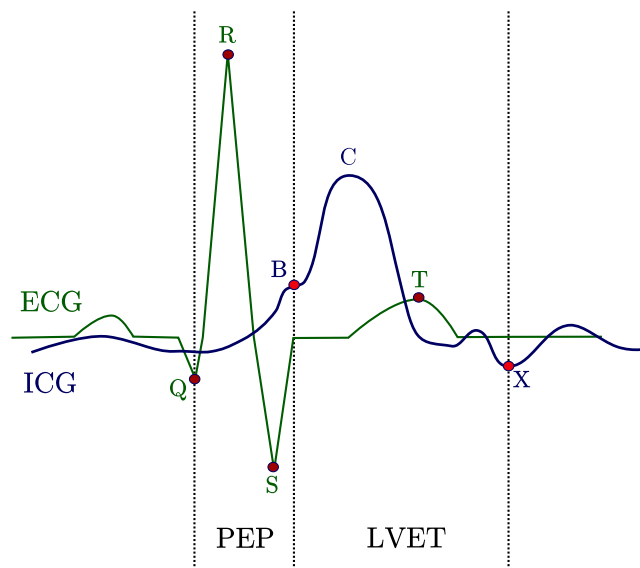


**FIGURE 1** Characteristic waveforms from ICG ( $\dot{z}(t)$ ) and ECG ( $v(t)$ ) during a single heartbeat. Key features such as the ICG B point and ECG QRS complex are labeled

Enthought's TraitsUI library for interactive plotting. The result is MEAP: the moving ensemble analysis pipeline.

We begin with a summary of the cardiovascular indices assessed in MEAP, followed by a rigorous definition of how electrophysiological recordings are turned into estimates of cardiovascular state when using traditional fixed-window ensemble averaging. We then describe our newly proposed moving ensemble averaging method, demonstrate the simplicity of preparing data for our method, and present illustrations that capture a rapidly changing set of cardiovascular signals.

## 1.1 | Cardiovascular measures

MEAP is designed to process and analyze data from the most common cardiovascular recording methods including ECG, ICG, BP, respiration, and pulse oximetry. Most of these data streams yield a continuous waveform that contains shape and amplitude features that reflect cardiovascular processes. These features must be identified in the waveform, either manually or through an algorithm, before their values can be used to calculate indices of cardiovascular functioning. For example, ICG and ECG waveforms accompanying a single heartbeat are plotted in Figure 1. While generally simple to identify visually, these waveform features and their relations can also be described mathematically.

For each heartbeat, the ECG R point serves as the  $t=0$  landmark for within-heartbeat events. Throughout this article, we define the corresponding heartbeat to begin at  $t = -200$  ms and end at  $t = 1,000$  ms relative to the R point, where ms = milliseconds. Let the ECG voltage time series

from the  $i$ th heartbeat be  $\mathbf{v}_i(t)$ . Thoracic impedance during a heartbeat  $i$  will be referred to as  $\mathbf{z}_i(t)$ . The  $\mathbf{z}_i(t)$  signal itself is not typically used for identifying critical points in the blood flow cycle. Instead, the first derivative of the ICG waveform ( $\dot{\mathbf{z}}_i(t) = \frac{d}{dt}\mathbf{z}_i(t)$ ) is used to facilitate the identification of key inflection points. Two key features of this derived ICG waveform, the B and X points (Figure 1), mark the opening and closing of the aortic valve, respectively. The time from the ECG Q point to the ICG B point defines the preejection period (PEP), which is related to the contractility of the heart muscle before blood is ejected. However, due to difficulty in reliably capturing the relatively small Q point, PEP is often calculated as the difference between the R point and the B point (the RBI), which is comparable to PEP in reliability (Kelsey et al., 1998, 2007) and validity (Kelsey et al., 1998; Mezzacappa et al., 1999), and is sensitive to predicted effects of task manipulations (Kelsey et al., 2000, 2004) and individual differences (Kelsey, 1991; Kelsey, Ornduff, McCann, & Reiff, 2001). This form of PEP is sometimes referred to as PEPr (Berntson, Lozano, Chen, & Cacioppo, 2004). This definition of PEP is also more robust for scoring data acquired during fMRI (Cieslak et al., 2015). Throughout this article and in the MEAP software, the RBI definition is used.

PEP is a particularly useful cardiovascular index as it is heavily influenced by the sympathetic nervous system, and thus is a primary measure used to assess task engagement, having been shown to vary with task difficulty and experience (Blascovich & Tomaka, 1996; Kelsey et al., 2004; Wright & Kirby, 2001). The ICG B and X points mark the beginning and end of left ventricular ejection. This interval is commonly called left ventricular ejection time (LVET). LVET can be used to calculate stroke volume (SV), the amount of blood ejected at a single heartbeat (Ebert, Eckberg, Vetovec, & Crowley, 1984). These estimates rely on a model of the torso as either a cylinder or cone. The most commonly used equation for SV was proposed by Kubicek, Patterson, and Witsoe (1970), calculating SV in milliliters for heartbeat  $i$  as

$$SV_i = \rho \times \frac{\ell^2}{Z_{0i}^2} \times \max(\dot{\mathbf{z}}_i(t)) \times LVET_i \quad (1)$$

where  $\rho$  is blood resistivity (typically set at a constant of 135 ohms cm),  $Z_{0i}^2$  is the square of the mean thoracic impedance between the B and X points of  $\dot{\mathbf{z}}_i$  (Kelsey & Guethlein, 1990),  $\max(\dot{\mathbf{z}}_i(t))$  is the maximum of  $\dot{\mathbf{z}}_i$  (i.e., the C point in Figure 1), and  $\ell$  is the distance between the thoracic voltage electrodes.

Cardiac output at beat  $i$  ( $CO_i$ ) is the amount of blood pumped in liters per minute, derived from both the ICG and ECG signal. The equation for cardiac output (Equation 2) is stroke volume (in mL/beat) multiplied by instantaneous heart rate (HR) in beats per minute, converted to liters per minute:

$$CO_i = HR_i \times SV_i / 1000. \quad (2)$$

Blood pressure is typically measured in psychophysiological studies as either SBP and DBP separately or combined into mean arterial pressure (MAP) as

$$MAP_i = \frac{1}{3}(2 \times DBP_i + SBP_i). \quad (3)$$

This blood pressure measure can be combined with ICG and ECG to estimate total peripheral vascular resistance (TPR):

$$TPR_i = 80 \text{ MAP}_i / CO_i, \quad (4)$$

which is in units of  $\text{dyne}/\text{cm}^2$  (Sherwood, Dolan, & Light, 1990).

## 1.2 | Ensemble averaging

Instead of marking these features and calculating these indices on individual heartbeats, it is both convenient and robust to ensemble average heartbeats occurring within experimentally relevant time windows. Suppose an experiment was run where participants sat still for 5 min with no task and then were exposed to randomized repetitions of two tasks, A and B, separated by a 30-s intertrial interval. Each task has  $k$  repetitions, each lasting  $m$  seconds. ECG, ICG, and BP are measured. A total of  $n$  heartbeats are detected during the experiment at times  $T_1, T_2, \dots, T_n$ . The ECG signal corresponding to heartbeat  $i$  is  $\mathbf{v}_i(t)$ . As defined earlier, let  $t$  represent the time within heartbeat, ranging from  $-200$  to  $1,000$  ms, with  $t = 0$  marking the R point. Time  $T_i$  is relative to the beginning of the physiological recordings. The following is a generalized notation that will be useful in comparing traditional ensemble averaging described in this section to our proposed moving ensemble averaging described in the next section. Using  $\mathbf{v}_i(t)$  and  $\mathbf{v}_j(t)$  as the ECG voltage time series for the  $i$ th and  $j$ th heartbeats, respectively, where  $i \neq j$ , the traditional ensemble averaged ECG signal for a single repetition of an experimental condition beginning at time  $\tau_0$  and ending at time  $\tau_1$  (such that  $\tau_1 - \tau_0 = m$ ) is calculated as follows:

$$\bar{\mathbf{v}}(t) = \sum_{i=1}^n \alpha(i) \mathbf{v}_i(t), \quad (5)$$

where  $\alpha(i)$  is a weight for heartbeat  $i$ ; calculated as

$$\alpha(i) = w(i, \tau_0, \tau_1) \left[ \sum_{j=1}^n w(j, \tau_0, \tau_1) \right]^{-1}, \quad (6)$$

such that

$$w(i, \tau_0, \tau_1) = \begin{cases} 1, & \text{if } \tau_0 \leq T_i \leq \tau_1 \\ 0, & \text{otherwise} \end{cases}. \quad (7)$$

Intuitively, traditional ensemble averaging starts by collecting data for all heartbeats occurring between  $\tau_0$  and  $\tau_1$  into a matrix:

$$\mathbf{V}_{(\tau_0, \tau_1)} = \begin{bmatrix} \mathbf{v}_k \\ \mathbf{v}_{k+1} \\ \vdots \\ \mathbf{v}_{k+p} \end{bmatrix}, \quad (8)$$

where the  $k$ th and  $(k + p)$ th heartbeats are the first and last heartbeats that occur inside the interval  $(\tau_0, \tau_1)$ , respectively.

The ensemble averaged ECG signal would then be the column means of  $\mathbf{V}_{(\tau_0, \tau_1)}$ , similar to the ERP method used for EEG analysis (Pfurtscheller & Lopes da Silva, 1999). The same procedure is followed for  $\dot{\mathbf{z}}$  and  $\mathbf{z}$ .

Once the ensemble averaged signals are computed, cardiovascular measurements are calculated on these ensemble averaged signals as if they were single heartbeats. The result is a single value for PEP, LVET, SV, CO, TPR for each epoch of interest. Each measure is then typically converted to a reactivity score by subtracting its value during the baseline condition. Traditional ensemble averaging is popular since one score per measure per fixed time window is a convenient format for a repeated measures analysis, which is typically the final stage of a physiological reactivity study. The final stage of the traditional ensemble averaging method usually consists of modeling each cardiovascular index separately using a repeated measures statistical analysis.

### 1.3 | Moving ensemble averaging

Our proposed approach, moving ensemble averaging, can be thought of as applying an ensemble averaging-like operation where, instead of averaging across the time epoch (by equally weighting all observations within the specified time epoch), a weighted ensemble average is calculated in a fixed window around every heartbeat. The weighting function corresponding to traditional ensemble averaging (Equation 7) is very similar to convolving a time series with a box kernel for smoothing. Box kernels of a specific width have the undesirable property of weighting the measurements from all time points within the window equally. When considering more flexible weighted averaging, alternative kernels such as Hanning or Blackman can be used to weight nearby time points more heavily while still incorporating more distal time points for de-noising purposes (Nuttall, 1981).

MEAP users can choose from a number of such weighting schemes; however, here we illustrate using a weighting function  $w_{lin}(i, j, \tau)$  that linearly downweights neighboring heartbeats according to their distance from the  $i$ th beat. Again, heartbeats are detected at times  $T_1, T_2, \dots, T_n$ . In our illustrations, a window of half-width  $\tau = 15$  s was used, meaning that a total of 30 s of neighboring heartbeats were included in the moving ensemble averaging. This value was chosen because we will later compare the moving ensemble averaged output to a 30-s fixed-window ensemble average.

For this initial MEAP paper, we chose the weighting function  $w_{lin}$  because of its illustrative simplicity. Other window functions and window lengths will be thoroughly explored and compared under different scenarios in future studies.

A set of heartbeats and their corresponding signals  $\mathbf{v}_i(t)$ ,  $\mathbf{z}_i(t)$ , and  $\dot{\mathbf{z}}_i(t)$  are run through the moving ensemble algorithm to produce a new, equal-sized set of signals,  $\hat{\mathbf{v}}_i(t)$ ,  $\hat{\mathbf{z}}_i(t)$ , and  $\hat{\dot{\mathbf{z}}}_i(t)$ . Note that influences on the impedance signals that are not synchronous with the ECG R wave, including low-frequency artifacts such as motion, speech, and changes in posture, are averaged out by the ensemble averaging process, and their effects will be minimized in the moving ensemble averaged waveforms.

The linearly weighted moving average formula is presented for ECG in Equation 9:

$$\hat{\mathbf{v}}_i(t) = \sum_{j=1}^n \alpha_{lin}(i, j) \mathbf{v}_j(t) \quad (9)$$

with

$$\alpha_{lin}(i, j) = \begin{cases} \frac{(1 - w_{lin}(i, j, \tau)/\tau)}{\left[ \sum_{k=1}^n (1 - w_{lin}(i, k, \tau)/\tau) \right]}, & \text{if } |T_i - T_j| \leq \tau \\ 0, & \text{otherwise} \end{cases} \quad (10)^1$$

where

$$w_{lin}(i, j, \tau) = |T_i - T_j|, \quad \text{if } |T_i - T_j| \leq \tau. \quad (11)$$

For example, suppose we want to calculate the weighting factor for a heartbeat  $j$  that occurs 5 s before heartbeat  $i$  using  $\tau = 15$  for the window half-width. The numerator of Equation 10 calculates how close  $T_j$  is to  $T_i$  as a fraction of  $\tau$ . The denominator sums over the analogous measures for all the heartbeats occurring in the  $\pm \tau$  interval around  $T_i$ . This guarantees that  $\sum_{j=1}^n \alpha_{lin}(i, j) = 1$ .

### 1.4 | Cardiovascular indices based on moving ensemble averaged heartbeat signals

Moving ensemble averaged heartbeats are used to produce a time series for each cardiovascular index. For example, SV values can be estimated at times  $T_1, T_2, \dots, T_n$ . The time series for each cardiovascular index can be examined for patterns evolving over time, or alternatively each time series could be summarized. For example, if the cardiovascular index values appear to change linearly over short intervals of time corresponding to an epoch of interest, one could summarize the pattern of change in the cardiovascular index using a

<sup>1</sup>[Correction added on 5 October 2017, after first online publication: Equation 10 has been amended.]

slope and intercept estimate as in simple linear regression. For example, suppose  $y(s)$  is a chosen cardiovascular index for  $s \in \{T_k, T_{k+1}, \dots, T_{k+p}\}$ , where times  $T_k, T_{k+p}$  mark the first and last heartbeats within the epoch of interest. Within MEAP, fitting the model

$$y(T_i) = \beta_1(T_i - \bar{T}) + \beta_0 + \varepsilon_i \quad (12)$$

leads to estimates of the rate of linear change of  $y(T)$  as  $\hat{\beta}_1$  and the intercept as  $\hat{\beta}_0$ , and provides the corresponding  $R^2$  value. Heartbeat times  $T_i$  are centered in Equation 12 for a more robust estimation of slope. For SV,  $\hat{\beta}_0, \hat{\beta}_1$  are in units of ml and ml/second, respectively. Estimates  $\hat{\beta}_0$  and  $\hat{\beta}_1$  for each of multiple time epochs of interest could subsequently be used in a repeated measures analysis to assess not only changes in the mean cardiovascular index ( $\hat{\beta}_0$ ) under different experimental conditions, but also in the mean rate of change ( $\hat{\beta}_1$ ).

It is important to note that the sequence  $T_1, \dots, T_n$  is specific to a single recording. Multiple separate recordings are typically created during an experimental session. Moving ensemble averaging is not reasonable across recordings if there is time between the acquisition of two consecutive tasks. In this manuscript, we calculate percent change against a short window of data immediately preceding the experimental events. It was therefore necessary that some task-free time was recorded at the beginning of each recording session. The events from multiple recordings can be analyzed together in the framework of a general linear model, as used commonly for multiscan fMRI analysis (Friston, Zarahn, Josephs, Henson, & Dale, 1999).

## 1.5 | MEAP software

MEAP was originally designed as a tool for analyzing large batches of cardiovascular data from multiple participants that was intuitive enough to be used by researchers without medical or engineering expertise. We automated as many parts of the pipeline as possible to reduce user error and increase reproducibility. Although many steps are automated, the interface requires the user to inspect the data at each step to confirm that processing was performed as expected. MEAP includes two tools: a preprocessing pipeline and an analysis interface.

### 1.5.1 | Software availability

MEAP runs on Windows 7 or greater, Mac OS X 10.10 or greater, and most recent, Linux distributions. Source code is released under the GNU General Public License version 2. Binary installers can be downloaded from <http://github.com/mattcieslak/MEAP/releases/>. Detailed instructions for installation along with a step-by-step tutorial for data processing and analysis are available in the online documentation at <http://meap.readthedocs.io/en/latest/>.

### 1.5.2 | MEAP pipeline interface

MEAP reads a Microsoft Excel file that specifies the locations of input files and their corresponding subject demographic and anthropometric data, such as distances between electrodes. Data files can also be imported manually, by right clicking within this window, selecting “import,” and navigating to the appropriate file. MEAP can currently read data from Acq-Knowledge (BIOPAC) or MATLAB formatted data. Figure 2a shows the MEAP logo and the top-level pipeline interface. Input data files are listed on the bottom left of the window. Files that have run through the pipeline to completion are colored light blue, while the currently active data file is highlighted in bold blue. The array of buttons on the right side of the window (magenta rectangle) shows the available processing steps in the pipeline, which remain grayed out until their prerequisite steps have been completed.

After importing data, the user then inspects the data to check for unusable segments of the recording. Such segments can be “censored” to be excluded from the rest of the pipeline, and measurements such as HR and heart rate variability are adjusted to reflect the censored intervals. Figure 2b depicts the “inspect data” interface. The black arrow highlights a small negative spike in the  $\dot{z}(t)$  signal where the user has decided to censor the data.

Before QRS detection, the user can apply a motion/respiration correction operation on the base impedance signal. Often speech and movement-related artifacts typically appear as a low-frequency perturbation in  $Z_0$ . MEAP’s approach to correcting these is to fit the  $Z_0$  time series with a series of Legendre polynomials and subtract the fitted time series from the data. The user may choose the order of polynomial regressors used during this step. The artifact-removed  $Z_0$  signal is then used throughout the rest of the pipeline. Note that a similar approach can be taken for other signals, such as blood pressure, during preprocessing.

Next, the user must detect and isolate each heartbeat. MEAP provides a number of options for this task, depending on the nature of the data. For relatively clean recordings, the default Pan-Tompkins algorithm (Pan & Tompkins, 1985) may be used. If the data were acquired during fMRI, there are two additional options. The first, called multisignal detection, finds heartbeat-related peaks in a simultaneously recorded non-ECG signal. For example, ICG and pulse oximetry have robust heartbeat-related peaks that are largely unaffected by fMRI-related noise. QRS complexes are searched for in time windows around peaks in the secondary signal. Finally, users may load a second ECG signal such as one collected by an EEG system. After one of these algorithms is run to detect QRS complexes, the user can manually add or remove QRS complexes as necessary. Figure 2c shows the QRS detection interface. Identified QRS complexes are displayed with a square at each apex. The arrow

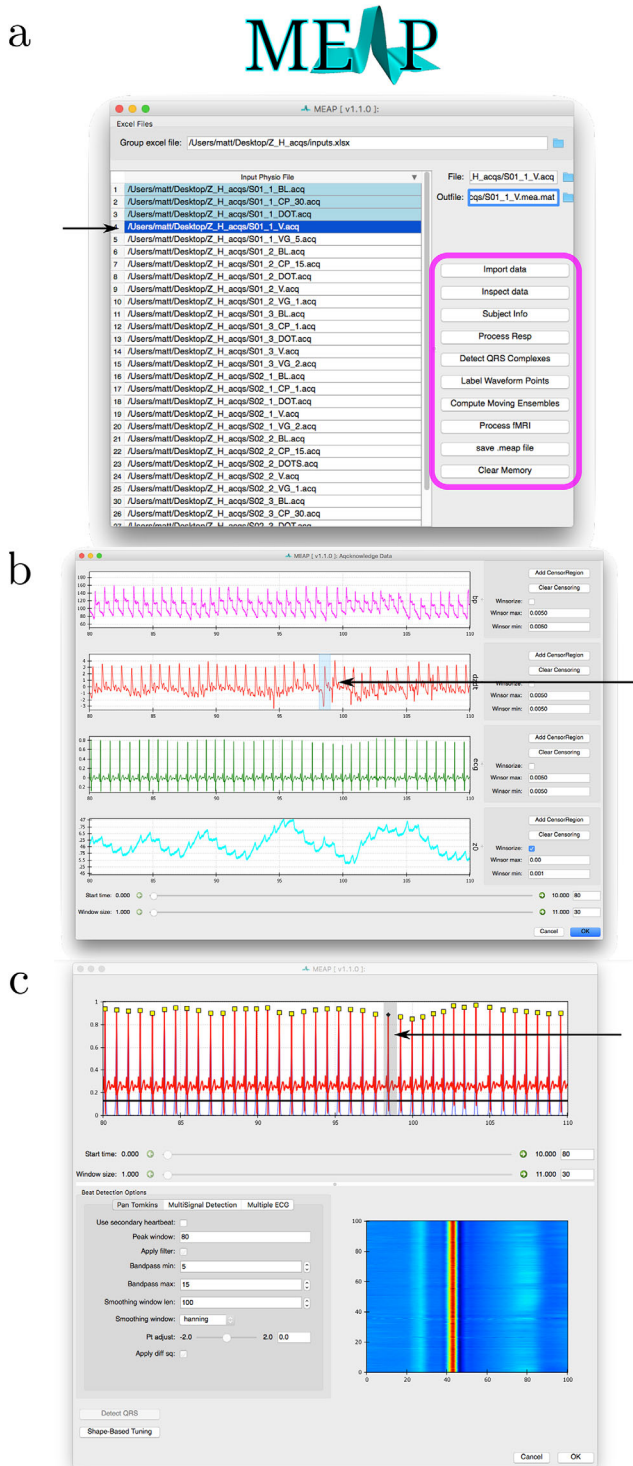


**FIGURE 2** First steps in the MEAP preprocessing pipeline. (a) MEAP logo and top-level pipeline interface. Left: input data files. Right: buttons corresponding to the steps in the processing pipeline. (b) “Inspect data” interface. Black arrow highlights a region in which the signal was censored. (c) QRS detection interface. Arrow highlights the censored region from (b). Black diamond at the R peak of this QRS complex indicates that this heartbeat should still be included in estimates of heart rate and heart rate variability but its corresponding  $\dot{z}(t)$  signal should not be included in any ensemble averaging. Bottom right: a matrix of all identified QRS complexes aligned at their R point (i.e., matrix in Equation 8)

highlights a grayed-out area that reflects the censored region from Figure 2b. The user has added a “do not ensemble” diamond marking to the R point of this QRS complex, meaning that the heartbeat should still be included in estimates of HR and heart rate variability but its corresponding  $\dot{z}(t)$  signal should not be included in any moving or traditional ensemble averaging. The bottom right panel within Figure 2c is a matrix of all identified QRS complexes aligned at their R points (i.e., the matrix in Equation 8). A mislabeled T wave, for example, will show up clearly in this plot, enabling the user to quickly hop to that location and manually fix the error.

After heartbeats have been identified, features on each waveform must be marked. MEAP initially presents the user with a plot of each signal ensemble averaged across the whole recording. The user checks that each feature has been correctly identified on these “global ensemble averages,” and the points will be marked on matching features on each individual heartbeat during subsequent analyses. The key exception is the ICG B point. The method employed to detect B points is described below.

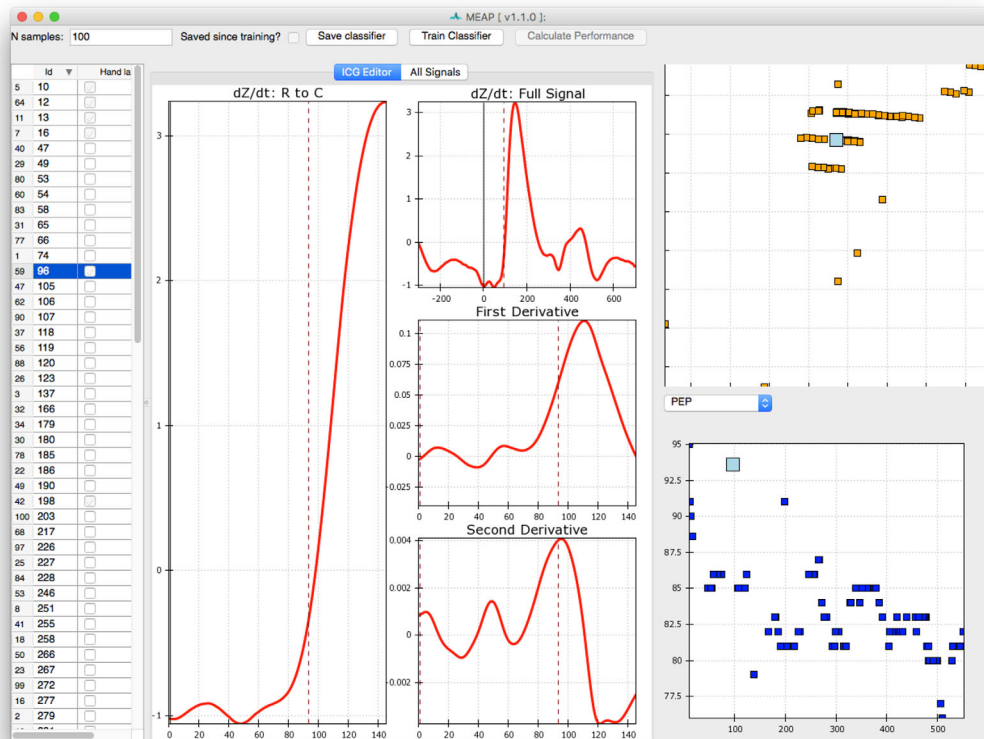
### 1.5.3 | B point classification algorithm

While most waveform features are easily located minima or maxima, the B point on the  $\dot{z}_i$  waveform can be difficult to mark (Debski, Zhang, Jennings, & Kamarck, 1993). Recent work has addressed the various methods currently employed to label this feature (Árbol et al., 2016), where specific peaks or zero-crossings of derivatives are compared to manual B point marking. MEAP implements many of the algorithms examined by that study, but also introduces a new classifier-based B point marking algorithm. Our algorithm begins by presenting the user with an interface where  $\dot{z}_i$  and its first two derivatives are displayed in a visual array. The user moves the cursor and clicks to select the B point. A random selection of heartbeats is selected by MEAP for manual marking in this manner (Figure 3a). These heartbeats are then used to train a classifier that can then be applied to all heartbeats (Figure 3).

Intuitively, we want to train a regression algorithm to take a short segment of a  $\dot{z}_i$  time series and identify how far (in time) the center of this segment is from the B point. For each hand-marked heartbeat, the algorithm examines the raw signal in fixed-size chunks surrounding each millisecond between the R point and the C point. Each of these chunks is paired with their distance (in milliseconds) from the hand-labeled B point, and the learning algorithm learns a function that maps feature vectors to times.

In our implementation, we extracted  $\dot{z}_i$  data in 41-ms chunks at 1 kHz and concatenated these chunks along with the first derivative of this time series into a feature vector

a



b

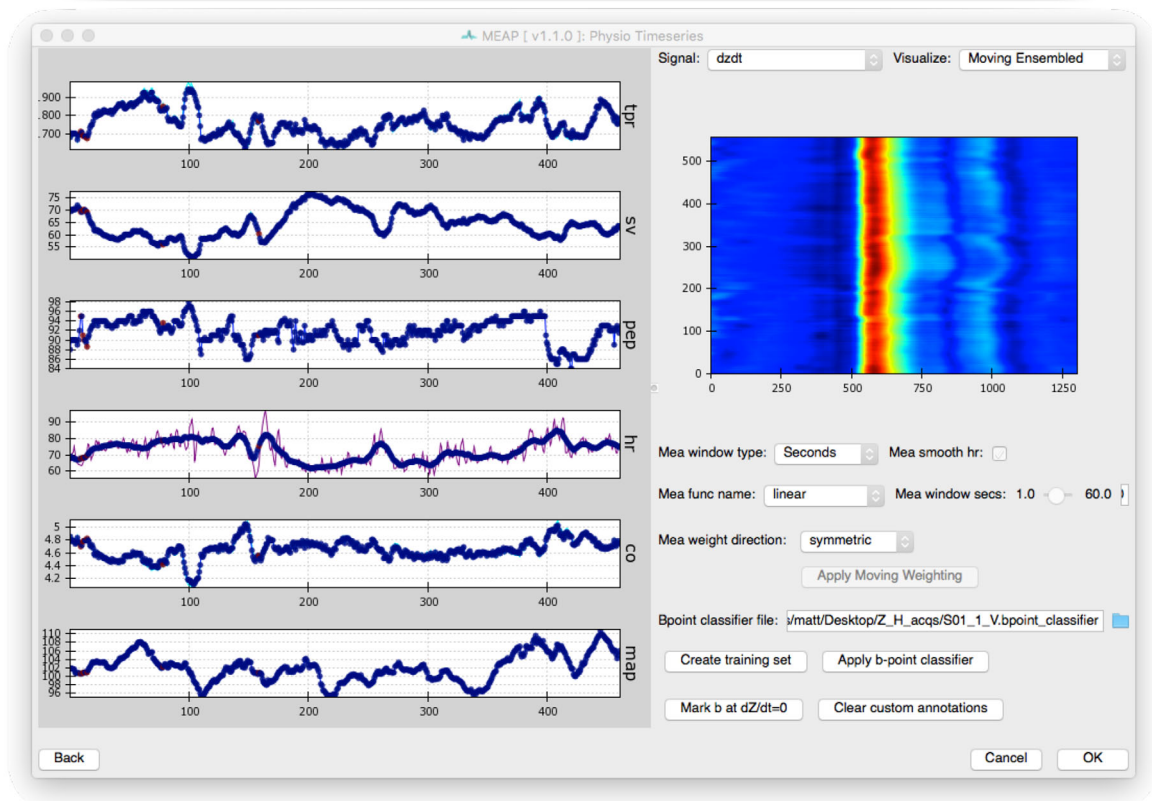
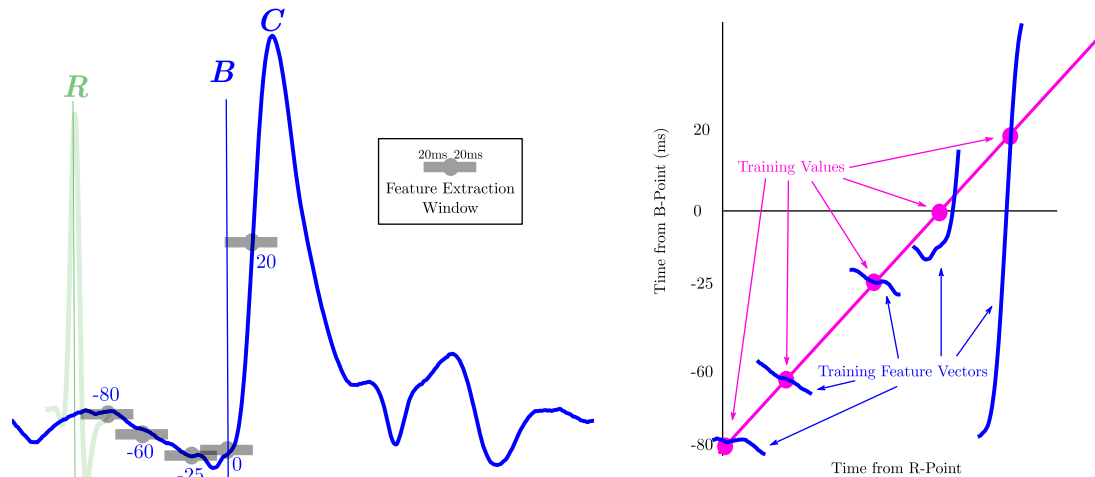


**FIGURE 3** (a) MEAP's B point training interface. The set of randomly selected heartbeats (left) lets users click a heartbeat that will then be displayed in the middle plot arrays. Bottom right: one user-chosen index out of SV, PEP, or LVET is plotted, and this panel is automatically adjusted as the user makes edits. Top right: systolic time intervals for all heartbeats are mapped to two dimensions and plotted. (b) Moving ensemble interface. Each cardiovascular index is plotted on the left versus time. User-specified parameters for moving ensemble averages ( $\tau$ ,  $\alpha$ , etc.) may be selected on the bottom right. A matrix of  $\hat{z}(t)$  is displayed as an image (top right), thereby illustrating how much temporal smoothing is introduced by the user's choice of parameters

## B-Point detection algorithm training



## Detecting the B-Point in new data

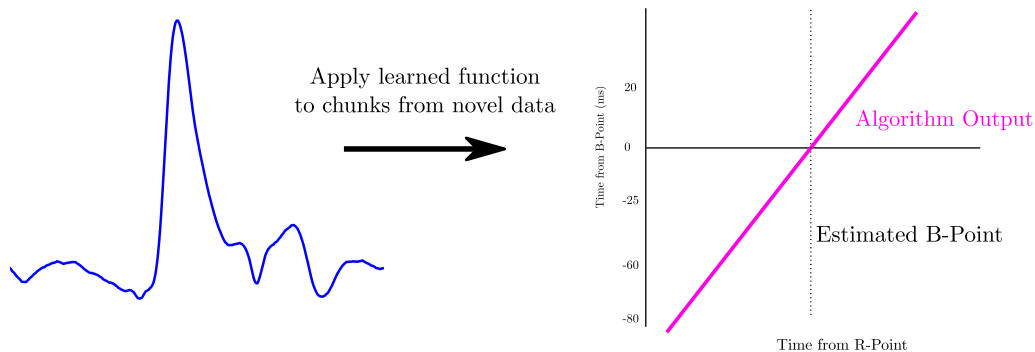


**FIGURE 4** Diagram of B point classifier algorithm. Top: Training procedure. Bottom: Learned mapping is applied to segments of data from unseen heartbeats, and the B point is marked as the value closest to zero in the outputs

(with a total of 82 total features). The B point detection algorithm is trained to match this feature with the distance in milliseconds of its center time from the B point. Each unseen  $\hat{z}_i(t)$  is then similarly converted to feature vectors for each millisecond between the R point and the C point. The learned function is applied to each feature vector, and the millisecond mapped closest to zero is marked as the B point. This procedure is illustrated in Figure 4.

The top half of Figure 4 depicts the training process. Hand-marked heartbeat  $i$ 's  $\hat{z}_i$  waveform ( $\hat{z}_i$ ) is plotted in blue. In order to train the classifier, each millisecond between the R point and the C point needs to be turned into a feature vector. At each millisecond  $t_k$  within the range of  $t = 0$  to the C point time, we extract the data from  $\hat{z}_i$  over the range  $\{t_k - 20 \text{ ms}, t_k + 20 \text{ ms}\}$ , providing a vector length of 41 ms. This operation is depicted in Figure 4 as a circle around  $t_k$  and a gray bar covering the  $\pm 20$  ms on either side for a few illustrative choices of  $t_k$ .

The top right panel shows these segments of  $\hat{z}_i$  on the x axis, which corresponds to the segment's time relative to the

R peak ( $t_k$ ), which is known. These segments are mapped to the y axis, which represents the distance in milliseconds between  $t_k$  and the B point for this heartbeat. B points subsequently are estimated for all heartbeats without hand-marked B points (shown in Figure 4, bottom) by similarly breaking each of these heartbeats up into feature vectors corresponding to each  $t_k$  between the R point and C point. The estimated distances from the B point,  $\hat{t}_k$ , are calculated by running each feature vector through the classifier and selecting the  $\hat{t}_k$  that is closest to 0. If multiple signal segments are equally close to 0, the mean is chosen as the B point, and a warning is printed into MEAP's log.

### 1.5.4 | Empirical demonstration of B point detection algorithm

For our first test case, we collected a large repeated measures ICG dataset. Each of 37 participants completed the same task procedures twice, one with measurements taken with traditional aluminum mylar bands and once with eight fMRI-

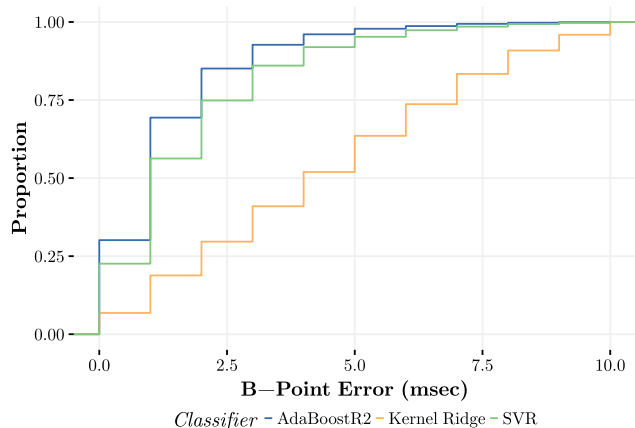


**FIGURE 5** Cumulative distribution functions of absolute errors are plotted for the best-performing B point identification algorithms. The height of each of the curves (step functions) at any chosen  $x$  shows the proportion of the 4,810 ICG waveforms that had  $x$  milliseconds of error or less based on the corresponding B point identification algorithm. The data are in 1-ms steps, as this is the resolution MEAP uses internally

compatible carbon fiber spot electrodes. Aluminum mylar bands were positioned according to the four-band array suggested by Sherwood et al. (1990). Carbon fiber electrodes were placed as suggested by Bernstein (1986). Each iteration of the task consisted of a 5-min resting baseline, a cold pressor task lasting up to 1 min, and a 2-min recovery period. All measurements in this first test case were taken with the participant in a supine position. ICG data were collected using BIOPAC's NICO100C-MRI amplifier, integrated using an MP150, and displayed and stored using AcqKnowledge software version 4.3 (BIOPAC, Goleta, CA) [Correction added on 5 October 2017, after first online publication: Equipment and software information have been amended.]. These data were ensemble averaged in 30-s fixed windows and manually annotated, resulting in 4,810 manually labeled  $\dot{z}(t)$  waveforms collected from these 37 participants.

Several candidate B point detection algorithms were tested on this dataset. These machine-learning algorithms all take a vector as input and learn a mapping to a scalar. We used implementations from Scikit-Learn (Pedregosa et al., 2011): support vector regression (Drucker, Burges, Kaufman, Smola, & Vapnik, 1997), kernel ridge regression (Murphy, 2012), and AdaBoostR2 (Drucker, 1997). Results are shown in Figure 5. In our studies, the top performing regression algorithm for B point marking among these three was AdaBoostR2 with a mean absolute error of  $1.3 \pm 1.5$  ms. AdaBoostR2 was therefore chosen as the default algorithm used in MEAP.

For our second test case, to evaluate the AdaBoostR2 B point detection algorithm performance on ICG measured on seated subjects, we ran 10-fold cross-validation on data from

two participants discussed further in the upcoming section “Empirical demonstration of MEAP.” Over a total of 2,820 hand-labeled B points, we observed a mean absolute error of  $0.93 \pm 0.98$  SD ms. The corresponding cumulative distribution function of detection errors is plotted in online supporting information Figure S2.

### 1.5.5 | MEAP analysis interface

The analysis interface allows the user to specify the design used in their experiment and calculates cardiovascular indices during each specified time period. These time periods and their corresponding preprocessed data files are specified in a Microsoft Excel file.

Figure 6 shows the result of loading preprocessed data into the MEAP analysis interface. The spreadsheet-like area in the top left of the window lists the user-specified time periods. The bright-blue highlighted row is the “active” experimental event for which ensemble averaged waveforms are displayed in the panel below. The user can adjust annotations by clicking and dragging within the plot. This allows the user to ensure that waveform features are correctly marked. Cardiovascular indices are updated in the spreadsheet view in real time.

The rightmost two plots show data colored by subject ID. The top right plot is the result of decomposing heartbeat feature arrays using independent components analysis and mapping each heartbeat based on its values for the first two independent components. The bottom right plot here shows the distance of the ICG B point from the ECG R point in milliseconds. Both of these plots are useful for identifying outliers, and clicking a point on either plot will cause the spreadsheet to jump to that time period's row and display the signals in the lower left plot.

Once the user has verified the quality of the heartbeat annotations, the results are written to a CSV file or Microsoft Excel spreadsheet. The final output contains a row for each event in the design file with columns added for all the calculable indices. Model fits and parameters from Equation 12 are also included. Output files can then be directly read into the user's preferred statistics software package.

## 2 | METHOD

### 2.1 | Empirical demonstration of MEAP

In order to demonstrate the utility of MEAP software and the moving ensemble average, we conducted a small longitudinal multiconditional study. Two female subjects, ages 19 and 21, completed a series of experimental tasks on three separate occasions over a 2-week period.

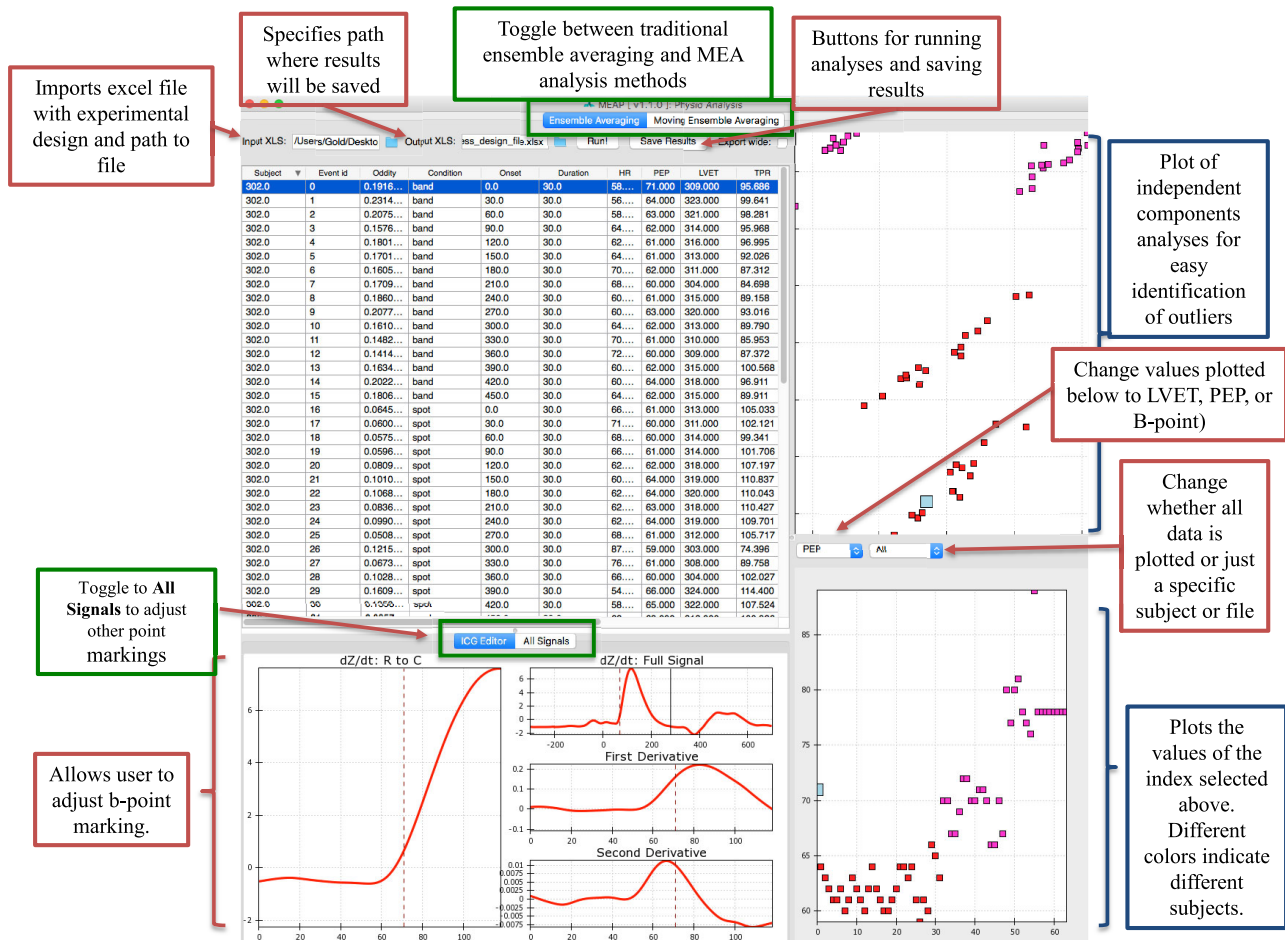


**FIGURE 6** MEAP interface for traditional fixed-window ensemble averaging analysis. The user preprocesses their data and loads a spreadsheet that points to the outputs and specifies experimental event onsets within them. These appear as rows in the spreadsheet to the top left. The rightmost two plots show data colored by subject ID and are designed to facilitate the detection of outliers within and between subjects

For this proof of concept, we selected a set of four tasks, including two frequently used physical stressors (the cold pressor and Valsalva) that are known to produce large and measurable responses (Gorlin, Knowles, & Storey, 1957; Kasagi, Akahoshi, & Shimaoka, 1995; Kelsey et al., 2007; Levin, 1966). These Valsalva (compression of the pelvic floor muscles) and cold pressor stressors were ideal for our purposes of illustrating MEAP's ability to describe the time-evolving patterns of change of a physiological measure, both within a participant and across participants. While the cold pressor and Valsalva tasks were chosen due to expected strong physiological changes, we also included two frequently used tasks for which we did not have prior reason to expect systematic physiological responses, namely, a video game and a random dot kinetogram task.

For this illustrative study, the order of three of the tasks (cold pressor, Valsalva maneuver, video game) was varied, as well as the order of the durations of each of the cold pressor (15, 30, 60 s) and video game (1, 2, 5 min) tasks. The random dot kinetogram task was completed

before or after the rest of the experimental trials of the experiment.

Each session began with a 5-min baseline recording. Subjects then completed each task, resting for 2 min between each. Physiological measures were recorded starting 30 s before the onset of the task or stressor, throughout the duration of the stressor, and over an additional 2-min recovery period following each task.

We quantified the similarity of the cardiovascular responses within each task by calculating the cross-correlation function (CCF). For each cardiovascular index (e.g., PEP, CO, etc.) the time series was resampled to 1 Hz and divided into subsets including the period starting 5 s prior to task onset and ending 25 s after task onset. Cross-correlation was used because differences in speed and force of the Valsalva maneuver can result in phase differences in the response. To quantify the similarity of these responses, we calculated the CCF between all six response time series (three per subject). The CCF maxima (and their corresponding time lags) were separated into two groups depending on whether the time series being compared came from the same

subject or different subjects. Complete code for performing these analyses is included in the supporting information. The mean of the CCF maxima should be close to 1 if the response time series are consistently shaped. Due to the small sample size, we refrain from performing significance tests.

To compare the moving ensemble method to current alternative methods, the Valsalva maneuver responses were analyzed in three different ways. We used MEAP with  $\tau = 15$ , then processed the data again with  $\tau = 0$ , equivalent to performing single-heartbeat analysis. Finally, we performed a traditional fixed-window ensemble averaging analysis.

## 2.2 | Experimental tasks

### 2.2.1 | Cold pressor

Cold pressor tasks are frequently used in hypertension research (Kasagi et al., 1995; Wood, Sheps, Elveback, & Schirger, 1984) and as a means of eliciting vasoconstriction in studies assessing the reliability of cardiovascular measures (Kelsey et al., 2007). Submerging the arm or foot in near-freezing water (Sherwood, Allen, Obrist, & Langer, 1986) or placing ice packs on the arm, foot, or forehead (Kelsey, Alpert, Patterson, & Barnard, 2000; Peckerman et al., 1991) has been shown to produce a reliable increase in TPR.

During an experimental session, each of the two participants completed a single cold pressor task lasting either 15, 30, or 60 s. Based on previous research (Kelsey et al., 2000; Peckerman et al., 1991) and in order to minimize movement, a folded “sandwich” of ice packs was slipped onto the participant’s hand for the amount of time specified by the trial. Each trial was separated by a recovery period of 2 min.

### 2.2.2 | Valsalva

The Valsalva maneuver, in which one attempts to force the contents of one’s lungs out through one’s nose while the airway is blocked, produces a baroreflex response associated with a cyclical changes in both stroke volume and vascular pressure. In healthy individuals with a normal cardiovascular system, the Valsalva maneuver produces a decrease in pulse pressure followed by an increase, overshooting the initial, resting MAP value once pressure is released. These cyclical changes are enacted to return the system to baseline and equalize blood flow to the brain and periphery under conditions of pressure changes. Due to these characteristic changes that the Valsalva maneuver evokes in healthy individuals, cardiovascular reactions to this maneuver have long been used to test cardiac function (Gorlin et al., 1957).

Participants completed a single Valsalva maneuver for approximately 3 s once during each of the three experimental sessions. Participants were instructed to take a deep breath and contract their abdominal/pelvic floor muscles for 3 s without exhaling. Every maneuver was followed by a relaxation period lasting 2 min.

### 2.2.3 | Video game

The video game was employed to elicit psychological stress rather than as a simple physical perturbation to the system. Participants played the video game “Crack-Attack,” a Tetris-like game in which ascending colored blocks are to be eliminated by aligning three or more of the same color by switching the blocks in the horizontal direction only (<http://crackattack.sourceforge.net>). The game was played on “extreme” mode, which greatly increased the speed of ascension and difficulty of the game and, hypothetically, the degree of psychological stress as well. Previous work has shown that a similar video game task reliably elicited significant cardiovascular changes from baseline (Kelsey et al., 2007). Each of the two participants played this game for 1, 2, or 5 min during each session, in random order.

### 2.2.4 | Random dot kinetogram task

The random dot kinetogram is a decision-making task that was implemented either before or after the other tasks. The task displays an array of mostly randomly moving dots, with a group of these dots moving together in a right or left direction (Britten, Shadlen, Newsome, & Movshon, 1992). The participant was told to distinguish whether this group was moving to the right or the left. This task thus served not as a stressor, but rather to measure cardiovascular state during a prolonged, repetitive perceptual task.

## 2.3 | Physiological measures and equipment

The physiological measures selected for this study were ECG, BP, and ICG—relatively standard measures of different aspects of the human cardiovascular system that can be used to evaluate physiological changes in participants due to perturbations to the system.

In order to assess ICG, a total of eight carbon fiber electrodes were placed on the neck and torso: two on each side of the neck and two on each side of the torso. Electrodes were placed identically to those in the cold pressor study (Bernstein, 1986).

Interelectrode distances were measured (between the inner pairs of electrodes) and recorded for later input into Equation 1 for calculation of SV and, subsequently, CO. ECG recordings were obtained using a modified Lead II

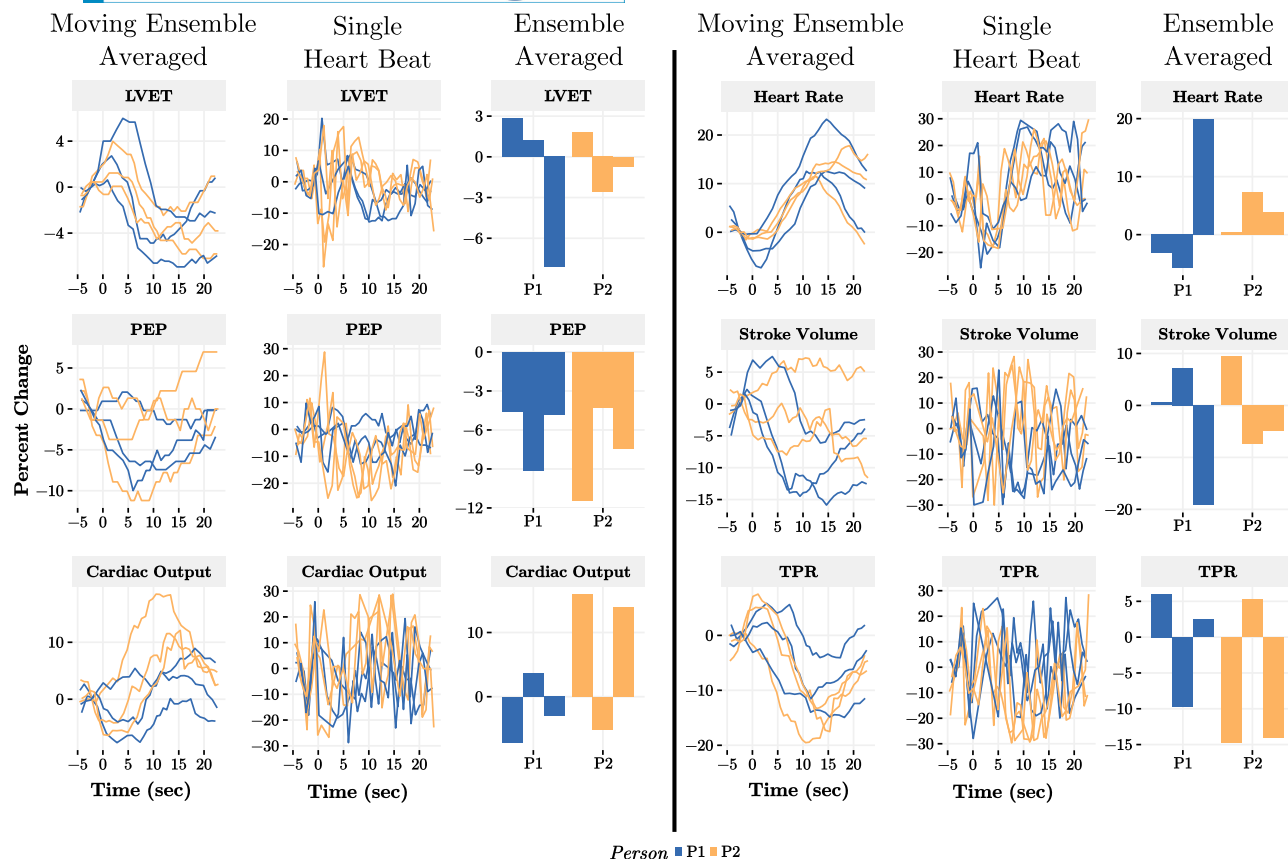


**FIGURE 7** Percent change in physiological measurements when a Valsalva maneuver was performed at  $t = 0$  on three separate occasions for each of participants P1 and P2. Cardiovascular measurements are divided into two side-by-side columns separated by a thick line, with each row depicting three different ways to measure the response to the Valsalva maneuver. The subcolumns depict, from left to right, the moving ensemble averaged time series, the raw signals with no averaging, and the fixed-window ensemble averaged response

configuration with sensors placed at the top of the sternum and at the bottom of the left pectoral muscle. The ICG electrodes provided the necessary ground.

Data were collected using the following equipment from BIOPAC (Goleta, CA): ECG was collected using an ECG100C-MRI amplifier, ICG using a NICO100C-MRI amplifier, and BP using the CNAP Monitor 500. Data were integrated using an MP150, and displayed and stored using AcqKnowledge software version 4.3 (BIOPAC) [Correction added on 5 October 2017, after first online publication: Equipment, software and manufacturer information have been amended.].

## 2.4 | The issue of baseline calculation

Cardiovascular reactivity analysis requires a baseline measurement. This is typically done by recording as the participant rests for at least a few minutes after electrodes are attached and before the tasks begin. Cardiovascular measurements are then examined to assess if they have stabilized over the baseline recording, and, if so, an average of the final few minutes of baseline will be used as the official baseline

value for that recording session. This approach has been used for decades, having been validated for numerous tasks (Kelsey et al., 2007). However, baseline measurements have been a thorny issue both theoretically and practically whenever hemodynamic measurements are studied (Stark & Squire, 2001). A true baseline is hard to define in a homeostatic system.

MEAP leaves baseline estimation and subtraction up to the user. All output is in absolute units. This enables the user to record and use a subject-specific explicit baseline condition, or to allow for the estimation of baseline within the framework of a mixed model. If the former approach is chosen, the user simply finds the baseline events in the output spreadsheet and subtracts their value from all experimental event measurements for that subject. The latter approach is particularly useful for event-related designs, as one can borrow tools from fMRI analysis where baseline often drifts over time (Lowe & Russell, 1999). Assuming that the onsets of experimental event types are evenly balanced across the recording, a drifting baseline can be incorporated into a linear mixed model as a set of orthogonal polynomials. Experimental event types are included in the design, and their coefficients are fit simultaneously to the drifting baseline.

## Cold Pressor

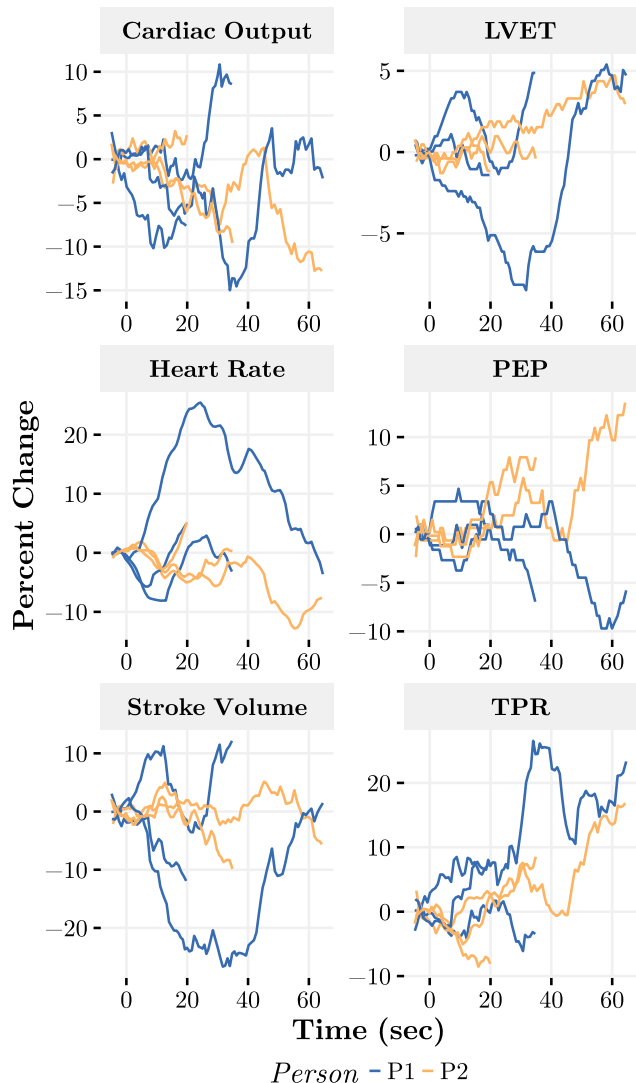


**FIGURE 8** Moving ensemble averaged physiological responses to the cold pressor. Percent change in physiological measurements when ice packs were applied to the hand that was not being used for blood pressure measurements is plotted for P1 and P2. The expected response (namely, increased TPR) is observed when the ice packs are applied for 60 s. Cold packs were applied for three different durations, resulting in different lengths of plotted data

Recently, a similar model has been proposed for characterizing event-related galvanic skin responses (Bach, Flandin, Friston, & Dolan, 2009).

We do not calculate reactivity against the 5-min baseline recordings taken at each session for the four tasks presented here. Instead, our presented percent change values are relative to the 5-s interval prior to the onset of the task. Additional repetitions and a balanced design would be necessary to perform a proper statistical analysis of these rapid physiological responses. Figure 7, 8, 9, and 10, along with the Discussion, are a purely illustrative demonstration of how cardiovascular state changes at the onset of a trial.

## 3 | RESULTS

### 3.1 | Comparison to existing methods

Responses to the Valsalva maneuver are quantified in three ways and displayed in Figure 7. Each row contains a cardiovascular index quantified by a different method in each of the two main columns. Traditional fixed-window ensemble averages (using 30 s) are shown as bar plots in the rightmost subcolumns of each main column because they yield a single value instead of a time series for each replication of the task.

The similarity of responses is quantified for the moving ensemble averaged data in the section below and for the single-heartbeat analysis in the supporting information Table S1. The fixed-window ensemble averages were not assessed

### Random dot kinetogram

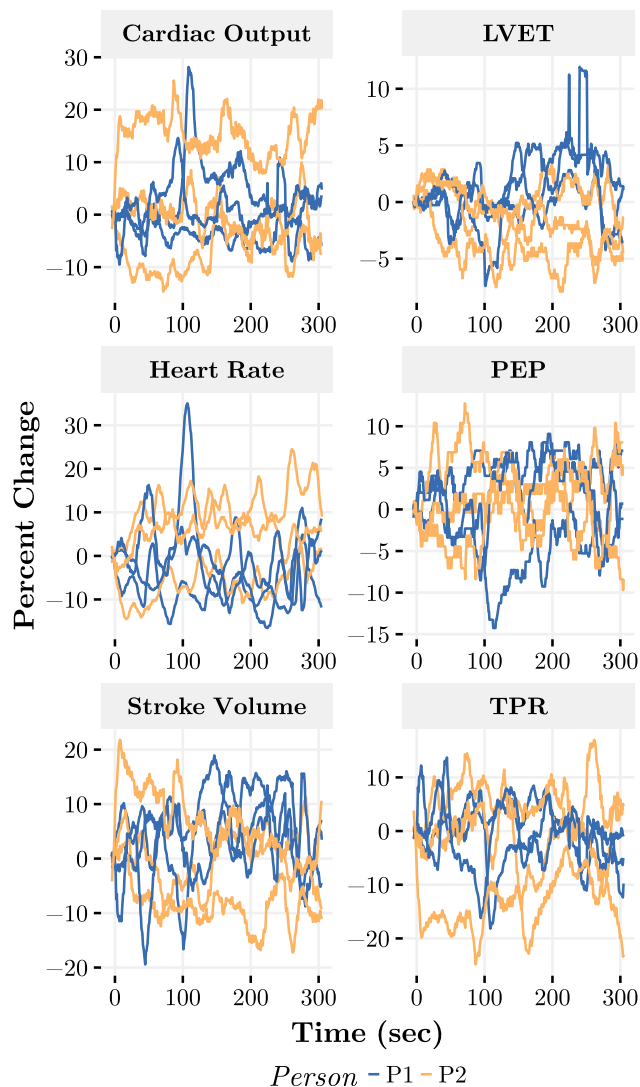


**FIGURE 9** Moving ensemble averaged cardiovascular time series during a 5-min random dot kinetogram task, for each of three sessions for each participant P1 and P2

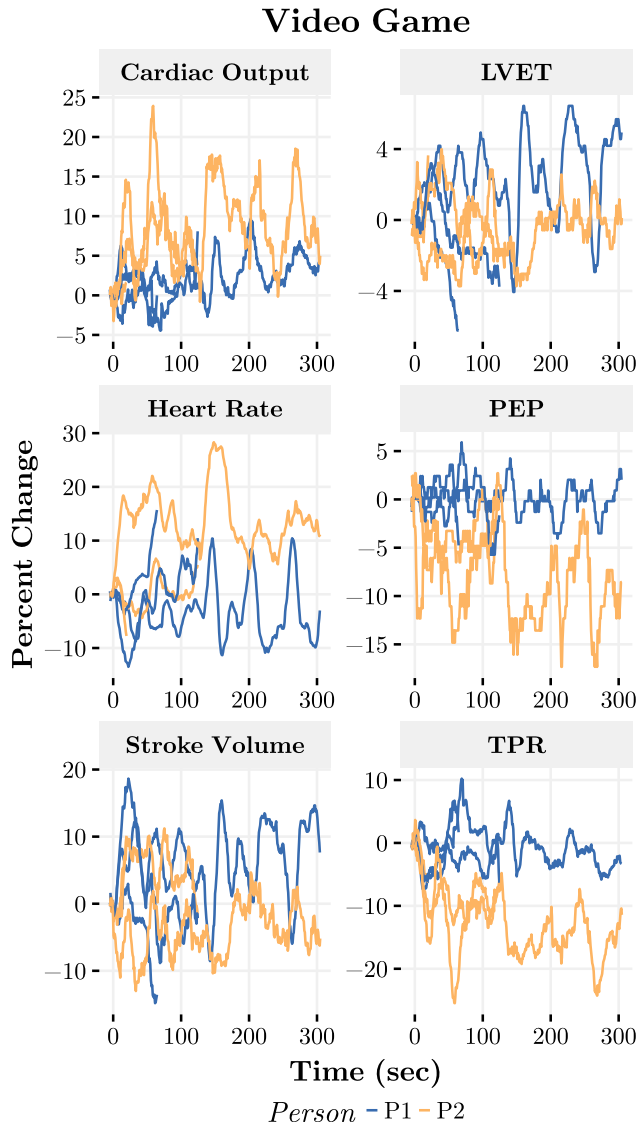


**FIGURE 10** Moving ensemble averaged cardiovascular time series during a video game

statistically since these only provide one value per task/session per subject for each of the CV measures.

In general, we see that the single-heartbeat analysis is noisier but finds larger percent change values. (Note that the vertical axes have different scales). The single-heartbeat response time series have overall lower cross-correlation coefficients (Table S1). The fixed-window ensemble averaged responses do not exhibit clear patterns for all variables except for PEP, which we see in the other methods has a relatively monotonic (negative) response to the Valsalva maneuver.

### 3.2 | Consistency across repetitions of the Valsalva maneuver

The Valsalva maneuver, a physical task, produces similar patterns of responses on certain cardiovascular measures

within and across individuals. These means are presented for each cardiovascular measure in Table 1. For reference, a correlation test of 31 samples with any of these correlation coefficients would result in a  $p$  value less than .01; however, it would not be valid to calculate  $p$  values on these mean CCF maxima directly, due to the small sample size. For this reason, these values should be interpreted primarily as a sanity check.

### 3.3 | Responses to different tasks

Responses to physical perturbations (Valsalva maneuver and cold pressor) are consistent with the known physiological responses to these tasks. The cold pressor produces a well-known rise in TPR in the trial where the ice was applied for 60 s (Figure 8). The Valsalva maneuver, although performed for only 3 s, produced clear examples of the baroreflex (Figure 7, left subcolumns): heart rate rapidly changes, leading to TPR changes, with associated changes in SV to counter the pressure from the maneuver. The baroreflex response is cyclic and rapidly changing. This illustrates the benefit of the finer time scale provided by the MEAP visualization, whereas a traditional ensemble average over the displayed 30-s period would have been at too coarse a time resolution to describe these rapid baroreflex changes.

**TABLE 1** Similarity of the cardiovascular response to the Valsalva maneuver as measured by the mean CCF maxima

Measure	Comparison	Mean CCF max	Mean lag (ms)
CO	Between	0.56 (0.18)	−0.89 (4.73)
	Within	0.45 (0.29)	4.67 (4.41)
HR	Between	0.63 (0.08)	0.11 (1.45)
	Within	0.61 (0.12)	−1.67 (1.37)
LVET	Between	0.78 (0.09)	−3.22 (2.28)
	Within	0.81 (0.10)	1.00 (2.37)
PEP	Between	0.80 (0.10)	0.78 (3.67)
	Within	0.80 (0.08)	2.00 (4.77)
SV	Between	0.61 (0.16)	−6.78 (3.31)
	Within	0.65 (0.26)	−2.00 (3.74)
TPR	Between	0.65 (0.34)	2.44 (3.84)
	Within	0.61 (0.34)	−2.17 (5.34)

*Note.* Standard deviations are reported in parentheses. The means and standard deviations of the time lags corresponding to the CCF maxima are also listed. CCF = cross-correlation function; CO = cardiac output; HR = heart rate; LVET = left ventricle ejection time; PEP = preejection period; SV = stroke volume; TPR = total peripheral vascular resistance.

We see considerably more variability during the cognitive tasks (Figure 9, 10). Cardiovascular indices varied substantially not only across individuals, but also substantially during repetitions of the same task within an individual. Since we did not record performance measures during these tasks, we could not relate performance to physiological state. Previous work has found that moving ensembled data from a pretask preparatory period can predict performance on the subsequent trial (Cieslak, 2016), so the lack of consistent response to cognitive tasks here may relate to the need for a more sophisticated experimental design to study task consistency. No behavioral data were collected during the video game task in this illustrative example. In future studies, it would be interesting to see if performance was affected by the dramatic changes observed within trials or if those changes were a reaction to events in the game.

## 4 | DISCUSSION

The moving ensemble averaging method presented here provides several advantages over traditional ensemble averaging methods and may represent a significant advancement in the field of cardiovascular assessment. First, and most obviously, this technique allows for the robust examination of near-continuous cardiovascular responses to discrete stimuli. The increased temporal resolution of the moving ensemble enables the assessment of variability within an individual across trials. It should be noted, however, that MEAP will not solve systematic problems introduced at data collection such as poorly attached electrodes, imbalanced designs, or trial-related systematic artifacts.

Some of the most popular tasks for inducing stress in a laboratory setting require participants to perform a speech in front of others (Kirschbaum, Pirke, & Hellhammer, 1993). Speech causes fluctuations in the  $Z_0$  signal that can impact estimates of stroke volume, and therefore cardiac output and TPR. Although the Valsalva maneuver includes respiration and muscle activity, it would be prudent to investigate robustness to speech in future work. For reference, previous research with tasks that involve speech and other activities has shown that fixed window ensemble averaging procedures are robust (Kelsey, 1991; Kelsey et al., 1998; Mezzacappa, Kelsey, & Katkin, 1999), suggesting that moving ensemble averaging may also perform well under such circumstances.

Statistically, the moving ensemble method recasts physiological reactivity as a time series problem. This has important implications for theories linking cardiovascular reactivity to motivation. Motivation can shift rapidly in relation to specific events and feedback (Quigley, Barrett, & Weinstein, 2002). For example, though an individual may display only a moderate threat response when averaged over the course of a GRE exam (<https://www.ets.org/gre>), he or

she may display cardiovascular reactivity characteristic of threat while solving difficult questions, but a pattern consistent with a challenged motivational state while answering easier items. The extent and duration of reactivity to specific questions may be a better predictor of overall performance than cardiovascular state averaged across the full exam. While multiple theories of motivation as well as emotion discuss the dynamic nature of appraisals (Blascovich & Tomaka, 1996; Frijda, Kuipers, & Ter Schure, 1989; Gross, 2002; Lazarus & Folkman, 1984), current methods for processing cardiovascular data have not allowed for their examination with sufficient resolution to assess physiological correlates of shifting appraisals as they occur in real time. The ability to track changes in cardiovascular responses with greater temporal resolution, and to model shifting baselines, is critical to increasing understanding of the relation between cardiovascular physiology and automatic appraisal processes (Blascovich, 2008). Conscious reappraisal, which has been shown to improve cardiovascular and cognitive responses to stress (Jamieson, Nock, & Mendes, 2012), is likely also a rapidly changing phenomenon.

Increasing the temporal resolution of key cardiovascular indices also has the advantage of facilitating their pairing with other time-varying signals. These signals may index physiological activity within the same person or an interaction partner. Within individuals, the simultaneous recording of cardiovascular reactivity and hemodynamic and/or electrical activity of the brain allows for time lag analyses to be conducted examining the temporal dynamics of communication between central and peripheral systems. Such methods may represent an important step in disentangling the role of peripheral and central nervous systems in the modulation of cardiovascular reactivity and behavior. Performing similar time lag analyses on cardiovascular data from two or more individuals may help elucidate the dynamics of emotional contagion (Hatfield, Cacioppo, & Rapson, 1993) and coregulation (Butler & Randall, 2013; Dezecache et al., 2013), and stress reactivity during intergroup interactions (Mendes, Blascovich, Lickel, & Hunter, 2002).

The moving ensemble estimates of cardiovascular indices demonstrated here are statistically similar to the blood oxygenation-dependent (BOLD) signal measured in fMRI. Early fMRI studies utilized block-design experiments—similar to those typically used with fixed-window ensemble averaging. The advent of so-called event-related fMRI designs not only allowed for estimation of responses to single trials, but the randomized order of events precluded potential confounds such as habituation, fatigue, and anticipation (Dale, 1999). Adopting a similar modeling strategy for ICG studies also allows for an estimation of baseline during intertrial intervals through a general linear model (Bach et al., 2009; Friston et al., 1999). Applying this method to cardiovascular data is likely to yield similar advances in the study of the peripheral systems as it did for the central nervous system.

## ORCID

Matthew Cieslak  <http://orcid.org/0000-0002-1931-4734>

## REFERENCES

- Árbol, J. R., Perakakis, P., Garrido, A., Mata, J. L., Fernández-Santaella, M. C., & Vila, J. (2016). Mathematical detection of aortic valve opening (b point) in impedance cardiography: A comparison of three popular algorithms. *Psychophysiology*, *54*, 350–357.
- Bach, D. R., Flandin, G., Friston, K. J., & Dolan, R. J. (2009). Time-series analysis for rapid event-related skin conductance responses. *Journal of Neuroscience Methods*, *184*(2), 224–234. <https://doi.org/10.1016/j.jneumeth.2009.08.005>
- Bernstein, D. P. (1986). Continuous noninvasive real-time monitoring of stroke volume and cardiac output by thoracic electrical bioimpedance. *Critical Care Medicine*, *14*(10), 898–901.
- Berntson, G. G., Lozano, D. L., Chen, Y.-J., & Cacioppo, J. T. (2004). Where to q in pep. *Psychophysiology*, *41*(2), 333–337. <https://doi.org/10.1111/j.1469-8986.2004.00156.x>
- Blascovich, J. (2008). Challenge and threat appraisal. In A. J. Elliot (Ed.), *Handbook of approach and avoidance motivation* (pp. 431–445). New York, NY: Psychology Press.
- Blascovich, J., & Tomaka, J. (1996). The biopsychosocial model of arousal regulation. *Advances in Experimental Social Psychology*, *28*, 1–52.
- Britten, K. H., Shadlen, M. N., Newsome, W. T., & Movshon, J. A. (1992). The analysis of visual motion: A comparison of neuronal and psychophysical performance. *Journal of Neuroscience*, *12*(12), 4745–4765. <https://doi.org/10.1.1.123.9899>
- Butler, E. A., & Randall, A. K. (2013). Emotional coregulation in close relationships. *Emotion Review*, *5*(2), 202–210. <https://doi.org/10.1177/1754073912451630>
- Cieslak, M. (2016). *Dynamics of the central and autonomic nervous systems preceding action and cognition* (Unpublished doctoral dissertation). University of California, Santa Barbara. Retrieved from ProQuest <http://www.proquest.com/>
- Cieslak, M., Ryan, W. S., Macy, A., Kelsey, R. M., Cornick, J. E., Verket, M., ... Grafton, S. (2015). Simultaneous acquisition of functional magnetic resonance images and impedance cardiography. *Psychophysiology*, *52*(4), 481–488. <https://doi.org/10.1111/psyp.12385>
- Dale, A. M. (1999). Optimal experimental design for event-related fMRI. *Human Brain Mapping*, *8*(2–3), 109–114. <https://doi.org/10.1111/spc3.12052>
- Debski, T. T., Zhang, Y., Jennings, J., & Kamarck, T. W. (1993). Stability of cardiac impedance measures: Aortic opening (B point) detection and scoring. *Biological Psychology*, *36*(1), 63–74. <https://doi.org/10.1111/psyp.12799>
- Dezecache, G., Conty, L., Chadwick, M., Philip, L., Soussignan, R., Sperber, D., & Grèzes, J. (2013). Evidence for unintentional emotional contagion beyond dyads. *PLOS ONE*, *8*(6), e67371. <https://doi.org/10.1371/journal.pone.0067371>
- Drucker, H. (1997). Improving regressors using boosting techniques. *ICML*, *97*, 107–115.
- Drucker, H., Burges, C. J., Kaufman, L., Smola, A. J., & Vapnik, V. (1997). Support vector regression machines. In M. C. Mozer, M. I. Jordan, & T. Petsche (Eds.), *Advances in neural information processing systems* (pp. 155–161). Cambridge, MA: MIT Press.
- Ebert, T. J., Eckberg, D. L., Vetovec, G. M., & Cowley, M. J. (1984). Impedance cardiograms reliably estimate beat-by-beat changes of left ventricular stroke volume in humans. *Cardiovascular Research*, *18*(6), 354–60. <https://doi.org/10.1093/cvr/18.6.354>
- Frijda, N. H., Kuipers, P., & Ter Schure, E. (1989). Relations among emotion, appraisal, and emotional action readiness. *Journal of Personality and Social Psychology*, *57*(2), 212–228. <https://doi.org/10.1037/0022-3514.57.2.212>
- Friston, K. J., Zarahn, E., Josephs, O., Henson, R., & Dale, A. M. (1999). Stochastic designs in event-related fMRI. *NeuroImage*, *10*(5), 607–619. <https://doi.org/10.1006/nimg.1999.0498>
- Gorlin, R., Knowles, J. H., & Storey, C. F. (1957). The Valsalva maneuver as a test of cardiac function: Pathologic physiology and clinical significance. *American Journal of Medicine*, *22*(2), 197–212. [https://doi.org/10.1016/0002-9343\(57\)90004-9](https://doi.org/10.1016/0002-9343(57)90004-9)
- Gross, J. J. (2002). Emotion regulation: Affective, cognitive, and social consequences. *Psychophysiology*, *39*(3), 281–291. <https://doi.org/10.1017/S0048577201393198>
- Hatfield, E., Cacioppo, J. T., & Rapson, R. L. (1993). Emotional contagion. *Current Directions in Psychological Science*, *2*(3), 96–100.
- Jamieson, J. P., Nock, M. K., & Mendes, W. B. (2012). Mind over matter: Reappraising arousal improves cardiovascular and cognitive responses to stress. *Journal of Experimental Psychology*, *141*(3), 417–422. <https://doi.org/10.1037/a0025719>
- Kasagi, F., Akahoshi, M., & Shimaoka, K. (1995). Relation between cold pressor test and development of hypertension based on 28-year follow-up. *Hypertension*, *25*(1), 71–76. <https://doi.org/10.1161/01.HYP.25.1.71>
- Kelsey, R. M. (1991). Electrodermal lability and myocardial reactivity to stress. *Psychophysiology*, *28*(6), 619–631. <https://doi.org/10.1111/j.1469-8986.1991.tb01005.x>
- Kelsey, R. M., Alpert, B. S., Patterson, S. M., & Barnard, M. (2000). Racial differences in hemodynamic responses to environmental thermal stress among adolescents. *Circulation*, *101*(19), 2284–2289. <https://doi.org/10.1161/01.CIR.101.19.2284>
- Kelsey, R. M., & Guethlein, W. (1990). An evaluation of the ensemble averaged impedance cardiogram. *Psychophysiology*, *27*(1), 24–33. <https://doi.org/10.1111/j.1469-8986.1990.tb02173.x>
- Kelsey, R. M., Ornduff, S. R., & Alpert, B. S. (2007). Reliability of cardiovascular reactivity to stress: Internal consistency. *Psychophysiology*, *44*(2), 216–225. <https://doi.org/10.1111/j.1469-8986.2007.00499.x>
- Kelsey, R. M., Ornduff, S. R., McCann, C. M., & Reiff, S. (2001). Psychophysiological characteristics of narcissism during active and passive coping. *Psychophysiology*, *38*(02), 292–303. <https://doi.org/10.1017/S0048577201000051>
- Kelsey, R. M., Reiff, S., Wiens, S., Schneider, T. R., Mezzacappa, E. S., & Guethlein, W. (1998). The ensemble-averaged impedance cardiogram: An evaluation of scoring methods and interrater reliability. *Psychophysiology*, *35*(3), 337–340. <https://doi.org/10.1017/S0048577298001310>
- Kelsey, R. M., Soderlund, K., & Arthur, C. M. (2004). Cardiovascular reactivity and adaptation to recurrent psychological stress: Replication and extension. *Psychophysiology*, *41*(6), 924–934. <https://doi.org/10.1111/j.1469-8986.2004.00245.x>

- Kirschbaum, C., Pirke, K.-M., & Hellhammer, D. H. (1993). The Trier social stress test—a tool for investigating psychobiological stress responses in a laboratory setting. *Neuropsychobiology*, *28*(1–2), 76–81. <https://doi.org/10.1159/000119004>
- Kreibig, S. D., Samson, A. C., & Gross, J. J. (2013). The psychophysiology of mixed emotional states. *Psychophysiology*, *50*(8), 799–811. <https://doi.org/10.1111/psyp.12064>
- Kubicek, W. G., Patterson, R. P., & Witsoe, D. A. (1970). Impedance cardiography as a noninvasive method of monitoring cardiac function and other parameters of the cardiovascular system. *Annals of the New York Academy of Sciences*, *170*(2), 724–732.
- Lazarus, R. S., & Folkman, S. (1984). Coping and adaptation. In W. D. Gentry (Ed.), *The handbook of behavioral medicine* (pp. 282–325). New York, NY: Guilford. <https://doi.org/10.1002/9781118453940>
- Levin, A. B. (1966). A simple test of cardiac function based upon the heart rate changes induced by the Valsalva maneuver. *American Journal of Cardiology*, *18*(1), 90–99. [https://doi.org/10.1016/0002-9149\(66\)90200-1](https://doi.org/10.1016/0002-9149(66)90200-1)
- Lovullo, W. R. (2005). Cardiovascular reactivity: Mechanisms and pathways to cardiovascular disease. *International Journal of Psychophysiology*, *58*(2), 119–132. <https://doi.org/10.1097/01.PSY.0000033128.44101.C1>
- Lowe, M. J., & Russell, D. P. (1999). Treatment of baseline drifts in fMRI time series analysis. *Journal of Computer Assisted Tomography*, *23*(3), 463–473.
- Matthews, K. A., Salomon, K., Brady, S. S., & Allen, M. T. (2003). Cardiovascular reactivity to stress predicts future blood pressure in adolescence. *Psychosomatic Medicine*, *65*(3), 410–415.
- Mendes, W. B., Blasovich, J., Lickel, B., & Hunter, S. (2002). Challenge and threat during social interactions with White and Black men. *Personality and Social Psychology Bulletin*, *28*(7), 939–952. <https://doi.org/10.1177/01467202028007007>
- Mezzacappa, E. S., Kelsey, R. M., & Katkin, E. S. (1999). The effects of epinephrine administration on impedance cardiographic measures of cardiovascular function. *International Journal of Psychophysiology*, *31*(3), 189–196. [https://doi.org/10.1016/S0167-8760\(98\)00058-0](https://doi.org/10.1016/S0167-8760(98)00058-0)
- Murphy, K. P. (2012). *Machine learning: A probabilistic perspective*. Cambridge, MA: MIT Press.
- Nuttall, A. (1981). Some windows with very good sidelobe behavior. *IEEE Transactions on Acoustics, Speech, and Signal Processing*, *29*(1), 84–91. <https://doi.org/10.1109/TASSP.1981.1163506>
- Obrist, P. A. (1981). *Cardiovascular psychophysiology*. Boston, MA: Springer. <https://doi.org/10.1007/978-1-4684-8491-5>
- Pan, J., & Tompkins, W. J. (1985). A real-time QRS detection algorithm. *IEEE Transactions on Biomedical Engineering*, *32*(3), 230–236. <https://doi.org/10.1109/TBME.1985.325532>
- Peckerman, A., Saab, P. G., McCabe, P. M., Skyler, J. S., Winters, R. W., Llabre, M. M., & Schneiderman, N. (1991). Blood pressure reactivity and perception of pain during the forehead cold pressor test. *Psychophysiology*, *28*(5), 485–495.
- Pedregosa, F., Varoquaux, G., Gramfort, A., Michel, V., Thirion, B., Grisel, O., ... Duchesnay, E. (2011). Scikit-learn: Machine learning in Python. *Journal of Machine Learning Research*, *12*, 2825–2830.
- Pfurtscheller, G., & Lopes da Silva, F. (1999). Event-related EEG/MEG synchronization and desynchronization: Basic principles. *Clinical Neurophysiology*, *110*(11), 1842–1857. [https://doi.org/10.1016/S1388-2457\(99\)00141-8](https://doi.org/10.1016/S1388-2457(99)00141-8)
- Quigley, K. S., Barrett, L. F., & Weinstein, S. (2002). Cardiovascular patterns associated with threat and challenge appraisals: A within-subjects analysis. *Psychophysiology*, *39*(3), 292–302. <https://doi.org/10.1017/S0048577201393046>
- Seery, M. D. (2013). The biopsychosocial model of challenge and threat: Using the heart to measure the mind. *Social and Personality Psychology Compass*, *7*(9), 637–653. <https://doi.org/10.1111/spc3.12052>
- Sherwood, A., Allen, M. T., Obrist, P. A., & Langer, A. W. (1986). Evaluation of beta-adrenergic influences on cardiovascular and metabolic adjustments to physical and psychological stress. *Psychophysiology*, *23*(1), 89–104. <https://doi.org/10.1111/j.1469-8986.1986.tb00602.x>
- Sherwood, A., Dolan, C. A., & Light, K. C. (1990). Hemodynamics of blood pressure responses during active and passive coping. *Psychophysiology*, *27*(6), 656–668. <https://doi.org/10.1111/j.1469-8986.1990.tb03189.x>
- Stark, C. E., & Squire, L. R. (2001). When zero is not zero: The problem of ambiguous baseline conditions in fMRI. *PNAS*, *98*(22), 12760–12766. <https://doi.org/10.1073/pnas.221462998>
- Wood, D. L., Sheps, S. G., Elveback, L. R., & Schirger, A. (1984). Cold pressor test as a predictor of hypertension. *Hypertension*, *6*(3), 301–306. <https://doi.org/10.1097/00007611-199503000-00010>
- Wright, R. A., Contrada, R. J., & Patane, M. J. (1986). Task difficulty, cardiovascular response, and the magnitude of goal valence. *Journal of Personality and Social Psychology*, *51*(4), 837–843. <https://doi.org/10.1037/0022-3514.51.4.837>
- Wright, R. A., & Kirby, L. D. (2001). Effort determination of cardiovascular response: An integrative analysis with applications in social psychology. *Advances in Experimental Social Psychology*, *33*, 255–307. [https://doi.org/10.1016/S0065-2601\(01\)80007-1](https://doi.org/10.1016/S0065-2601(01)80007-1)

## SUPPORTING INFORMATION

Additional Supporting Information may be found online in the supporting information tab for this article.

### Table S1

### Figure S1

### Appendix S1

**How to cite this article:** Cieslak M, Ryan WS, Babenko V, et al. Quantifying rapid changes in cardiovascular state with a moving ensemble average. *Psychophysiology*. 2018;55:e13018. <https://doi.org/10.1111/psyp.13018>